COMMUNICATION

ChemComm
www.rsc.org/chemcomm

Ultrathin hollow nanoshells of manganese oxide

Lianzhou Wang, Yasuo Ebina, Kazunori Takada and Takayoshi Sasaki†*

Advanced Materials Laboratory, National Institute for Materials Science, 1-1 Namiki, Tsukuba, Ibaraki 305-0044, Japan. E-mail: sasaki.takayoshi@nims.go.jp

Received (in Cambridge, UK) 12th February 2004, Accepted 16th March 2004
First published as an Advance Article on the web 1st April 2004

Novel hollow nanoshells of Mn_2O_3 with controllable ultrathin shell thickness have been fabricated through layer-by-layer assembly of exfoliated MnO_2 nanosheets and polyelectrolytes on polymer bead templates, followed by removal of the polymer cores *via* calcination.

Manganese oxides have been extensively investigated as catalysts, ion exchangers, and electrocatalysts.[1] It is generally recognized that their performance is highly dependent on their morphologies as well as crystallographic forms. A wide variety of morphological forms of manganese oxides, ranging from single crystals and thin films to nanowires, nanosheets, and nanoparticles, have been reported.[1–6] Very recently, Suib *et al*. reported that a controlled reaction of $MnSO_4$ and $HMnO_4$ yielded a new form of γ-MnO_2 showing catalytic potential.[7] Microporous manganese oxide flakes were self-aggregated to form a skeletal object having hollow openings. However, few studies have mentioned the formation of hollow shells with a balloon-like spherical morphology.

Inorganic hollow shells with well-defined architectures are of increasing interest due to their low density, high surface area, stability, and surface permeability; they may find a wide range of applications as catalysts, shape-selective adsorbents, chemical sensors, and capsules for controlled release of therapeutic agents.[8] Hollow shells of a variety of inorganic materials, including ceramic oxides, non-oxides, and metals, have been prepared to date.[8–13] We recently reported the fabrication of hollow shells of titanium oxide using $Ti_{0.91}O_2$ nanosheets as shell building blocks or "wrapping paper" onto a sacrificial template,[14] demonstrating the advantages of such an approach: nearly spherical ultrathin shells with a smooth surface can be obtained owing to the highly flexible and two-dimensional nature of the nanosheets, which are ~1 nm thick. Here we report on the rational fabrication of hollow nanoshells of Mn_2O_3 through layer-by-layer (LBL) coating of exfoliated MnO_2 nanosheets and polyelectrolyte onto polymer beads and subsequent calcination. The unilamellar nanosheets effectively cover the surfaces of the polymer templates, yielding so-called core–shell composites. The hollow shells which are obtained upon calcination of the composites show a well-defined spherical architecture (diameter: 350–380 nm) and the shell walls are ultrathin (10–15 nm).

A colloidal suspension of exfoliated MnO_2 nanosheets was synthesized by employing our recently reported procedure.[5b] The resulting negatively charged MnO_2 nanosheets have a crystallographic thickness of 0.5 nm and a lateral size of several hundred nanometers, as demonstrated in our previous study.[5b] A positively charged polyelectrolyte (polyethylenimine, PEI) was used as a binder and commercially available poly(methyl methacrylate) (PMMA) spheres (400 nm in diameter) were employed as template cores. A typical procedure for the alternate LBL assembly of PEI and MnO_2 nanosheets was conducted as follows: PMMA beads (0.3 g) were ultrasonically dispersed in 100 cm^3 of H_2O containing 0.02 g of PEI and then stirred for 15 min to precoat the PMMA surface with PEI, followed by centrifuging (6000 rpm, 10 min) and washing with water to remove excess PEI. The next MnO_2 layer was adsorbed by re-dispersing the PEI-coated PMMA beads in 100 cm^3 of H_2O and then adding the colloidal suspension of MnO_2 nanosheets (10 cm^3, concentration: 0.8 g dm^{-3}) dropwise under stirring. This procedure yielded flocculated sediment as a result of the electrostatic interaction of the nanosheets and PMMA beads. The products were recovered by washing with water and centrifuging. Core–shell composites coated with multilayer shells of $(PEI/MnO_2)_n$ were prepared by repeating the above procedures *n* times. The as-prepared composites were finally calcined at 450 °C in air to yield hollow nanoshells of manganese oxide.

The growth of (PEI/MnO_2) shells was readily identified by the change in color of the PMMA beads. White powders changed to light and then dark brown as the number of coating layers of colored MnO_2 nanosheets increased. Diffuse reflectance UV-visible spectra for the recovered core–shell composites indicated a marked change, revealing a pronounced absorption characteristic of MnO_2 nanosheets,[5b] even after a single coating cycle (Fig. 1), indicating the adsorption of MnO_2 nanosheets onto the PMMA beads. X-Ray powder diffraction (XRD) data [Fig. 2(a)] for the composites provide evidence for the progressive growth of multilayer shell structures. A broad feature in the 2θ range 10–20° is attributable to the amorphous halo from PMMA. Its intensity was appreciably diminished upon coating of inorganic nanosheets. The XRD peak at a 2θ value of 7.3°, indicated by an arrow, is ascribed to PEI/MnO_2 layer pairs with a repeating distance of *ca*. 1.2 nm. Considering the crystallographic thickness of MnO_2 nanosheets (0.5 nm), the PEI layers must therefore be about 0.7 nm in thickness, in agreement with the value reported in the film systems.[15] Two additional peaks in the higher 2θ range are assignable to intrasheet reflections of 10

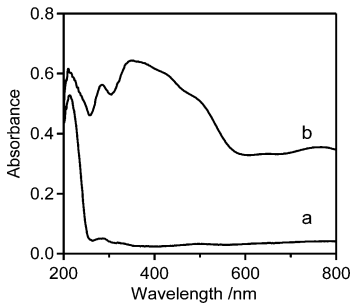

Fig. 1 Diffuse reflectance UV-visible spectra of bare PMMA (a) and core–shell composites recovered after the first PEI/MnO_2 coating cycle (b).

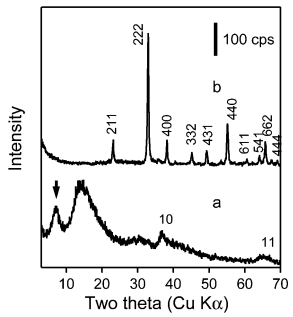

Fig. 2 XRD patterns of core–shell composites with 20 PEI/MnO_2 layer pairs (a) and hollow nanoshells obtained by calcination of the composites at 450 °C (b). The arrow in (a) indicates the XRD peak with a repeating distance of 1.2 nm.

† CREST, Japan Science and Technology Agency (JST).

DOI: 10.1039/b402209b

and 11 bands from a two-dimensional hexagonal cell (a = 0.28 nm) for MnO_2 nanosheets,[16] confirming that the nanosheet architecture remained intact. These XRD profiles are enhanced with increasing numbers of coats, providing a strong indication that the alternate LBL assembly of PEI and MnO_2 nanosheets on the PMMA surfaces operates successfully. Similar diffraction features have been observed in the shell assembly of titania nanosheets on polymer spheres.[14] The formation of core–shell structures was also observed by scanning electron microscopy (SEM). After 20 coating cycles, the core–shell particles retained the spherical form of the original polymer beads, except for some slight irregularities [Fig. 3(a) and (b)]. This feature clearly indicates the feasibility of core–shell formation using highly flexible nanosheets as shell building blocks. Note that shape deformation of the spherical nanocomposites may occur due to thermal damage to the polymer cores caused by the SEM electron beam.

The core–shell composites coated with 20 bilayers of PEI/MnO_2 underwent a weight loss of 88% upon heating up to 400 °C. The major weight loss, together with a huge exotherm, occurred in the range 200–300 °C, which is attributable to combustion of the template cores. Because a negligible loss was observed above 400 °C, suggesting the complete decomposition of the template, the core–shell composites were calcined at 450 °C to remove the PMMA cores. The XRD pattern [Fig. 2(b)] of the resulting products can be indexed as a pure phase of Mn_2O_3 (JCPDS, no. 65-1798), indicating the phase transformation from MnO_2 nanosheets to Mn_2O_3. Calcination of the composites at higher temperatures resulted in the collapse of the hollow nanoshells and the formation of an Mn_3O_4 phase.

The hollow nature and nearly homogeneous spherical curvature of the calcined nanoshells was confirmed by transmission electron microscopy (TEM) imaging [Fig. 3(c)]. The diameter of the hollow shells ranges from 350 to 380 nm, indicating that only limited shrinkage took place during the heat treatment. The high magnification image reveals a shell thickness of 10–15 nm [Fig. 3(d)]. As mentioned above, the thickness of the MnO_2 nanosheets is ~0.5 nm. Consequently, the net thickness of 20 layers of stacked nanosheets after removal of the PEI layers is expected to be ~10 nm (20 × 0.5). This is consistent with the TEM observations, strongly suggesting that our strategy was successful in rationally controlling the shell thickness with subnano- to nanometer precision. The hollow nanoshells that are the final product are very light, like tiny feathers or snowflakes, and move with a slight external force, reflecting their low apparent density due to the ultrathin shells and high diameter/shell thickness ratio. The BET specific surface area of the hollow nanoshells was determined to be 113 $m^2\ g^{-1}$, which is considerably higher than that of the Mn_2O_3 obtained in nanoparticle form[17] and is comparable with that of skeletal hollow materials composed of molecular sieve flakes.[7] If we consider that the hollow nanoshells are composed of perfect shells with a diameter of 350–380 nm and a thickness of 10 nm, a theoretical net surface area for the material should be around 80 $m^2\ g^{-1}$,‡ *i.e.* slightly lower than the experimentally determined value. This deviation may be reasonably ascribed to the contribution of the inner porosity of the shells. The features of a well-defined hollow architecture and high surface area may mean that this material has potential as a catalyst.

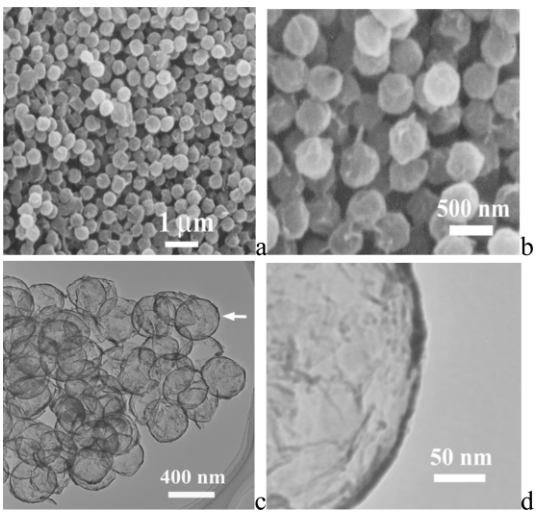

Fig. 3 Low (a) and high magnification (b) SEM images of core–shell composites prepared with 20 layer pairs of PEI/MnO_2. (c) TEM image of hollow nanoshells obtained after calcination of composites coated with 20 layer pairs. (d) High magnification TEM image showing the wall structure of the area marked by arrow in (c).

In summary, hollow nanoshells of Mn_2O_3 have been fabricated *via* sequential adsorption of PEI and exfoliated MnO_2 onto PMMA spheres and subsequent calcination. The nanoshells have controllable shell thickness and a defined architecture, and show promise for applications in catalysis and electrochemistry.

Notes and references

‡ The volume, weight, and surface areas (inner and external areas) of a single perfect hollow nanoshell were calculated by taking its diameter, shell thickness, and a density of 5.03 g cm^{-3} for Mn_2O_3, then the theoretical surface area in $m^2\ g^{-1}$ was estimated.

1 (*a*) S. L. Brock, N.-G. Duan, Z.-R. Tian, O. Giraldo, H. Zhou and S. L. Suib, *Chem. Mater.*, 1998, **10**, 2619; (*b*) Q. Feng, H. Kanoh and K. Ooi, *J. Mater. Chem.*, 1999, **9**, 319.
2 X.-J. Yang, W.-P. Tang, Q. Feng and K. Ooi, *Cryst. Growth Des.*, 2003, **3**, 409.
3 (*a*) Y. Lvov, B. Munge, O. Giraido, I. Ichinose, S. L. Suib and J. F. Rusling, *Langmuir*, 2000, **16**, 8850; (*b*) L. Z. Wang, Y. Omomo, N. Sakai, K. Fukuda, I. Nakai, Y. Ebina, K. Takada, M. Watanabe and T. Sasaki, *Chem. Mater.*, 2003, **11**, 2873.
4 (*a*) Q.-M. Gao, S. L. Suib and J. F. Rusling, *Chem. Commun.*, 2002, 2254; (*b*) X. Wang and Y.-D. Li, *J. Am. Chem. Soc.*, 2002, **124**, 2880.
5 (*a*) Z.-H. Liu, K. Ooi, H. Kanoh, W.-P. Tang and T. Tomida, *Langmuir*, 2000, **16**, 4154; (*b*) Y. Omomo, T. Sasaki, L. Z. Wang and M. Watanabe, *J. Am. Chem. Soc.*, 2003, **125**, 3568.
6 M. Yin and S. O'Brien, *J. Am. Chem. Soc.*, 2003, **125**, 10 180.
7 J.-K. Yuan, K. Laubernds, Q.-H. Zhang and S. L. Suib, *J. Am. Chem. Soc.*, 2003, **125**, 4966.
8 F. Caruso, *Chem. Eur. J.*, 2000, **6**, 413.
9 K. Kamata, Y. Lu and Y.-N. Xia, *J. Am. Chem. Soc.*, 2003, **125**, 2384.
10 C. E. Fowler, D. Khushalani and S. Mann, *Chem. Commun.*, 2001, 2028.
11 A. Dong, N. Ren, Y. Tang, Y.-J. Wang, Y.-H. Zhang, W.-M. Hua and Z. Gao, *J. Am. Chem. Soc.*, 2003, **125**, 4976.
12 X. Wang, Y. Xie and Q.-X. Guo, *Chem. Commun.*, 2003, 2688.
13 S. W. Kim, M. Kim, W. Y. Lee and T. Hyeon, *J. Am. Chem. Soc.*, 2002, **124**, 7642.
14 L. Z. Wang, T. Sasaki, Y. Ebina, K. Kurashima and M. Watanabe, *Chem. Mater.*, 2002, **14**, 4827.
15 T. Sasaki, Y. Ebina, T. Tanaka, M. Harada and M. Watanabe, *Chem. Mater.*, 2001, **13**, 4661.
16 L. Z. Wang, K. Takada, A. Kajiyama, M. Onoda, Y. Michiue, L. Q. Zhang, M. Watanabe and T. Sasaki, *Chem. Mater.*, 2003, **15**, 4508.
17 Q. Zhao and W. H. Shih, *Microporous Mesoporous Mater.*, 2002, **53**, 81.